PEER REVIEWED

Quantitative evaluation of the forming jet delivered from four different hyraulic headboxes using high speed digital imaging

CYRUS K. AIDUN

ABSTRACT

Hydraulic headboxes have many different forms and shapes with some similar design features and some significantly different parts. The tubes in the tube bank have different geometries and arrangements. Some headboxes have sheets inside that extend from the tube bank to several inches from the slice. The author uses earlier outlined methods to examine the forming jet delivered by four different headboxes. The combination of these covers most features available in hydraulic headboxes. The paper examines the hydrodynamic characteristics of the forming jet for each machine and discusses the relation between observed features in the forming jet and the headbox structure.

Application: *Consideration of the relationship of featuring in the forming jet and the headbox can help to eliminate defects in papermaking.*

THIS STUDY EXAMINES THE forming section of four paper making machines using high speed digital imaging and image processing techniques. In each case, images are taken of the headbox slice and the forming layer just after the impingement line. Side and overhead views are taken of all machines. Overhead views contain the most quantitative information and are the focus of image processing routines *(1)*. **Figures 1 and 2** and **Tables I and II** outline the regions of the forming section imaged in each case.

The purpose of this study was to implement the high speed imaging methods to analyze various commercial headbox and forming sections. Considering the variety of headbox and forming sections, the author selected four machines that cover the different design features most popular in commercial headboxes. The paper also includes two headboxes having similar designs for comparison of the imaging method. The machines all have fourdrinier forming sections with easy access for side and top views. During the imaging studies, these commercial machines operating under different parameters, but all produced base sheet coated paper. **Table III** presents the relevant operational parameters for each machine.

A digital video system captures the dynamics of the streaks on the forming table. Off-line image processing analysis and signal analysis techniques quantified the scale and regularity of the streaks *(1)*. To help the comparison of one paper making machine to another, plotting of the data uses similar scales, and the printed image data have overlaid grids. The following text presents and discusses fast Fourier transform (FFT) for the averaged images and the time series images. Comparing FFT data across machines is possible by plotting the ratio of standard deviation to the average value.

RESULTS AND ANALYSIS

In the imaging of the forming jet and the forming layer, this work focused on the fluid dynamics after the impingement line region. Despite these attempts, accessing and recording the images at the same relative distance from the slice and the impingement line was not possible. This was due to the differences in the headbox slice design and the location of the catwalk on the forming table. For accurate documentation, this work noted in careful records the exact location on the forming table imaged. Figures 1 and 2 show the typical overhead view layout and a map of the locations where each machine was imaged. Figure 2 outlines the distance from the imaging region to the slice. Tables I and II show the range of the forming table covered in the imaging study and the position of the samples. For machines A and B, imaging the forming jet before the impingement line was not possible. In the comparison of the images, this work therefore focuses on the region after the impingement line for all cases.

The four fourdrinier paper machines considered in this study operate under similar conditions. Since they are commercial, the operating parameters are different. Table III summarizes these parameters using data provided by the mill.

Some parameters have a range with an estimate of the operating value. In those cases, the note below the table specifies the range. Some parameters from the mill were not accurate measurements.

Earlier work has outlined the steps for enhancing an image *(1)*. **Figure 3** a–d shows typical enhanced images of the forming jet for machines A–D, respectively. These images used 0.06 millisecond expo-

Machine	Start of close image	End of close image	Start of far image	End of far image
A	11.5	23.4	28.8	42.3
B	4.0	21.5	-	-
C	-1.1	6.1	13.0	20.1
D	0.0	5.0	9.0	17.4

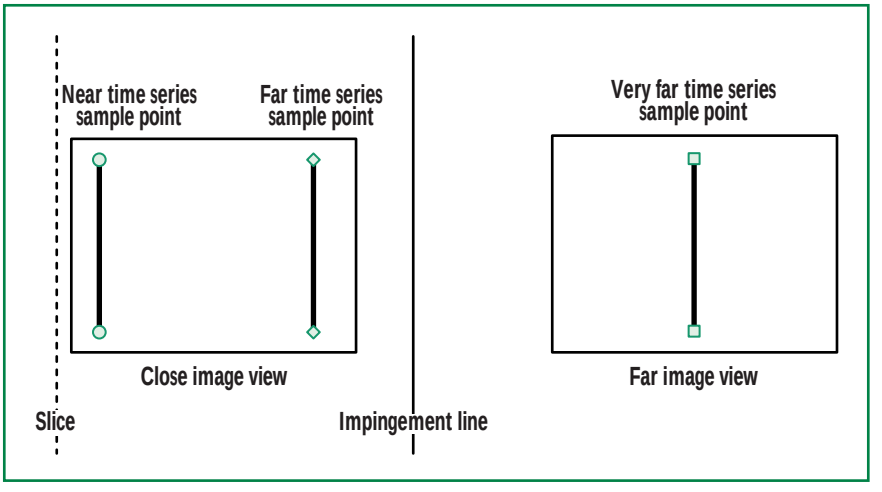
I. Averaged images—range of table covered, in. from slice

Machine	Near	Far	Very Far	Impingement line
A	12.8	20.9	35.5	4.0
B	7.0	15.5	-	4.0
C	0.5	3.5	16.5	4.8
D	0.5	4.5	13.5	5.5

II. Time series images—positions of samples, in. from slice

sure time at 1000 images per s. A 1000 W tungsten light illuminated the forming jet from the side of the forming table. The streaks in the forming jet reflect the incident light at varying intensity to the camera depending on the nonuniform curvature of the liquid surface. In principal, these images allow calculating the amplitude of the streaks or waves from the intensity of the recorded light. This approach does require a more precise control on the light intensity. This is a requirement not easily achieved in the mill during a commercial run without interference with the operation and production of the machine.

Visual inspection of the images in Fig. 3 provides some view of the forming jet characteristics. One can immediately see slight nonuniformities in cross direction (CD) and machine direction (MD) in all the forming layers. Jet roughness and small structures in the forming jet result from turbulent flow inside the headbox and the mean secondary flows. The scale of the surface roughness seen on the forming layer in Fig. 3 relates to the turbulent eddy size and strength. Some similarities exist between images for machines A and B. Machines C and D have very similar features and show a similar forming layer pattern after the impingement line. The impingement angles in these machines are different. The degree of stock jump after impingement should therefore be different. This study is more concerned about the surface pattern and regularity of the flow on the forming table. Comparison of the A and B forming layers, in Fig. 3 a and b with the C and D forming layers in c and d of the same



1. Typical overhead view layout showing image positions and time series sample points

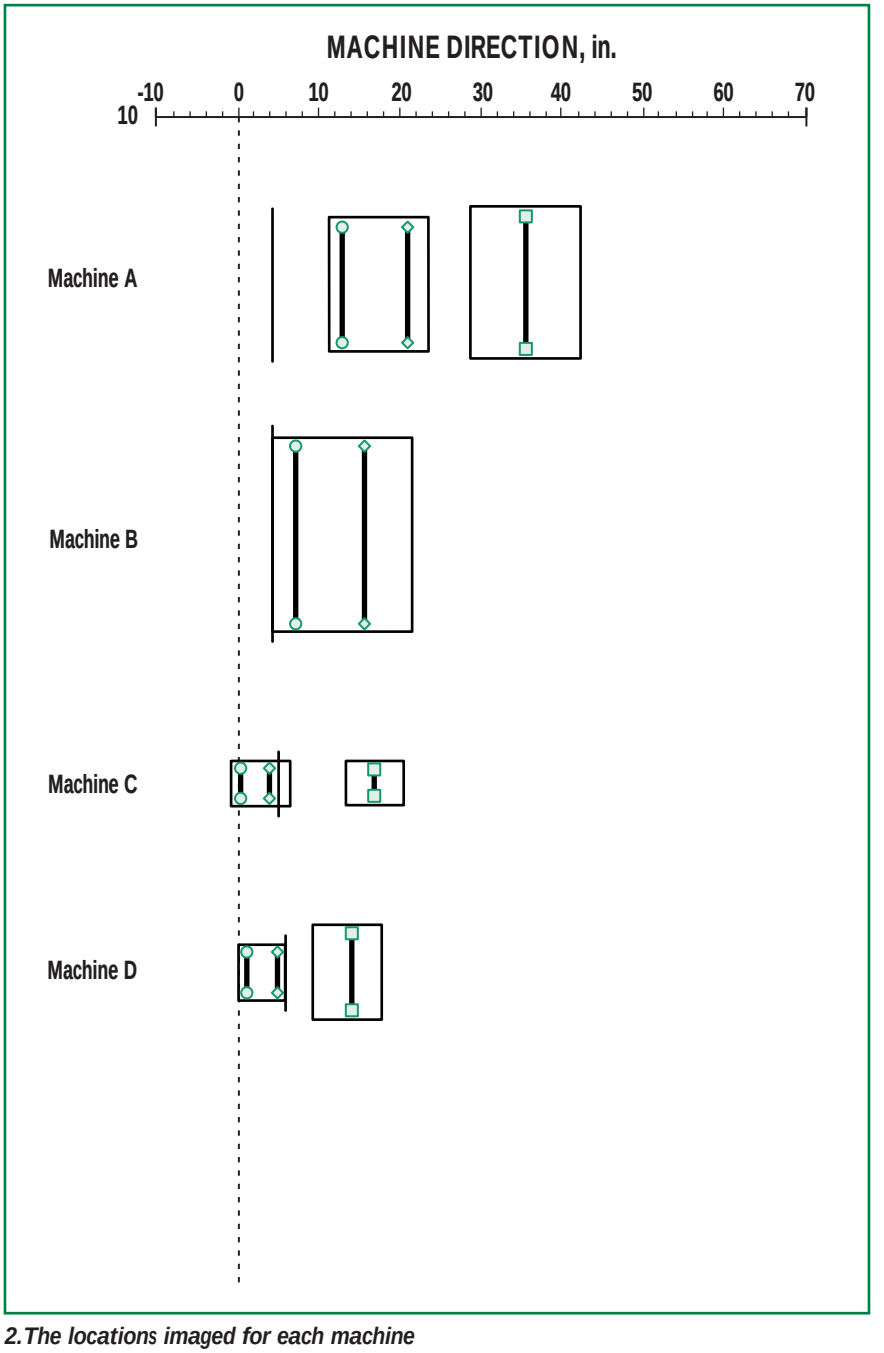
Machine	Machine width, in.	Headbox flow rate, gal/min	Wire speed, ft/m³	Rush, drag	Consistency	Slice opening, in.
A	332	18,992	2917	0.997	0.61	0.45[2]
B	234	-[1]	2640	0.992	0.65	0.55[2]
C	265	17,808	3000	-[3]	0.90	0.55[4]
C	302[5]	-[6]	-[1]	1.005[8]	-[9]	0.49[10]

1. Not reported
2. These values may not be very accurate (± 10%)
3. Not reported
4. Given as vertical = 0.55 in. and horizontal = -0.46
5. Given as wire = 302 in., slice =294 in., and reel = 272 in.
6. Range given as 16,000–24,000
7. Range given as 2000–3400
8. Given as J/W = 1.005
9. Range given as 0.40–0.75
10. Range given as 0.4–0.6 in., typical value listed in table

III. List of parameters for the four paper machines studied

figure reveal a fundamental difference in pattern. The A and B layers show a jagged streaky pattern where the C and D layers show a straight streak in the machine direction. The reason for this difference is a fundamental difference between machine A and B headboxes and the headboxes on machines C and D.

The headbox on machine A has one tube bank, an inclined tube column, and vanes or sheets between the rows of tubes. Headbox B also has one tube bank with a regular vertical column and vanes or sheets between the tube row. Machines C and D have almost identical headboxes. They have a set of manifold tubes, a "stilling chamber," and three rows of staggered tubes in the second bank of tubes before the converging nozzle. No vanes or sheets



2. The locations imaged for each machine

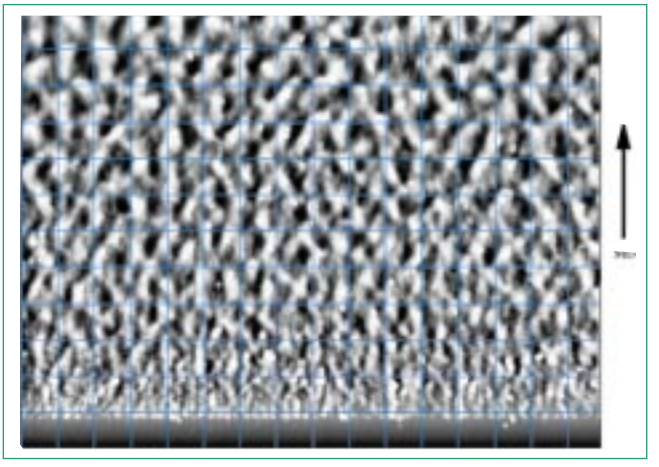
exist inside the converging nozzle of the C and D headboxes.

KEYWORDS
Defects, digital techniques, fluid dynamics, fluid mechanics, forming sections, fourdrinier machines, head boxes, hydrodynamics, image analysis, jets, mechanics, paper machines, streaking, water streaks.

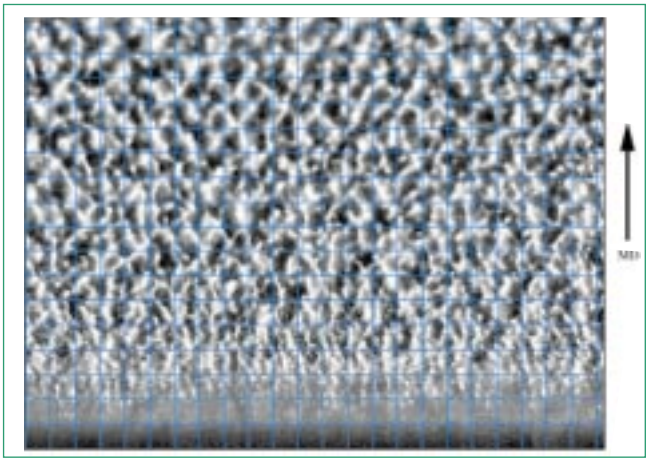
As outlined elsewhere *(2)*, the interaction of the jets from the tubes inside the headbox generates mean secondary flows that result in a regular streak pattern on the forming table. The jets from the tubes are squeezed onto neighboring jets below and above generating mean secondary flows as counter rotating vortices. With headboxes A and B, the sheets delay the interaction of the jets in this manner.

The question arises whether the streak patterns seen in Fig. 3 are only due to random turbulent fluctuations of the flow inside the headbox or to a deterministic streak pattern. To investigate this, this work averaged the flow over 0.1 s—100 frames—to give the results in Fig. 4 a–d for machines A–D, respectively. Deterministic streak patterns are obvious in all cases, although case B shows much noise or random variations in the averaged image. The grid line superimposed on the images represents a 1-in. length scale. Evaluating the degree of "regularity" of the streaks cannot rely on the visual inspection of these images or the averaged images. A quantitative method of evaluation requires computing the average and the standard deviation of the FFT of each CD scan line of the mean image averaged over 100 frames—the image presented in **Fig. 4** a–c for each machine and averaged over 300 frames for Fig. 4 d. More regular and persistent streaks have smaller standard deviation of the FFT divided by the mean value of the FFT. A rigorous evaluation needs to compare using equal headbox and forming section parameters. This means equal slice opening, machine speed, average jet velocity, jet impingement angle, and the ratio of the average jet velocity to the wire speed. Finding two machines that operated with the same values of these parameters was not possible. The four machines in this study were the closest to the ideal case.

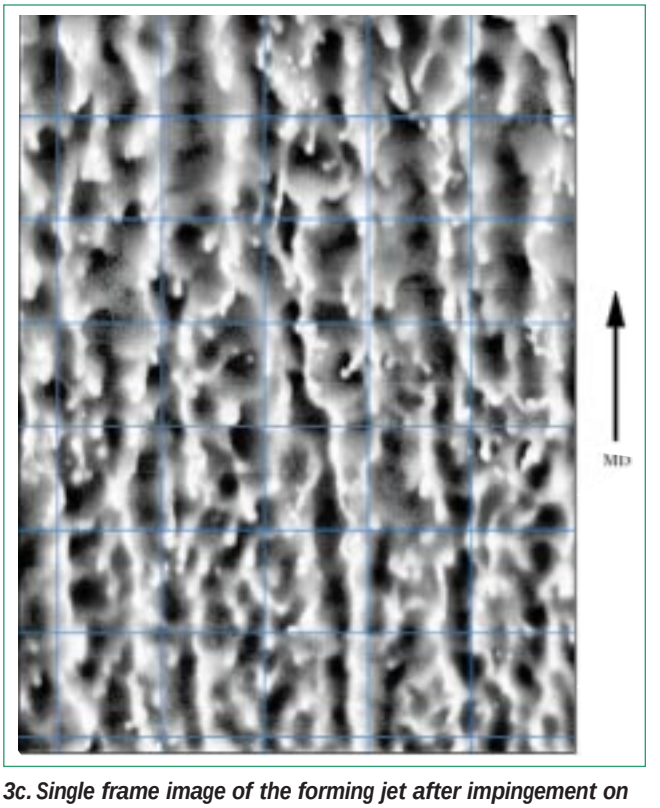
With the understanding that the difference in the operational parameters listed in Table III between these machines could influence the quantitative results. **Figures 5 and 6**, respectively, present the comparison of the FAT standard deviation divided by averaged FAT for 100 and 500 frames—0.1 and 0.5 S. Inclusion of the 500 frames averaged FFT results demonstrates that the number of frames considered in this evaluation-



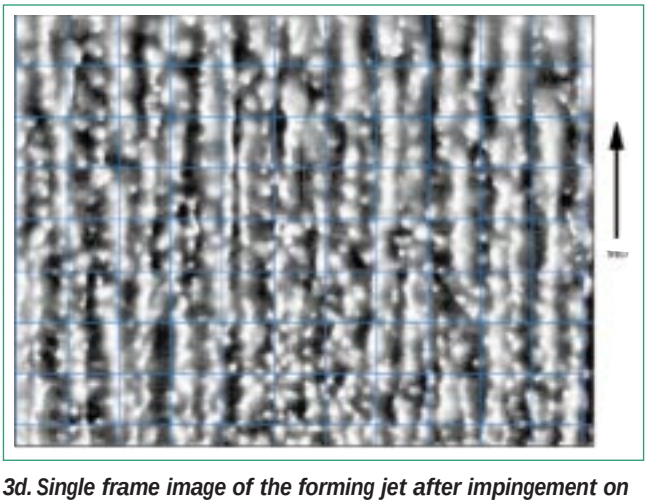
3a. Single frame image of the forming jet after impingement on the forming wire of machine A with gridlines showing a 1-in. length scale



3b. Single frame image of the forming jet after impingement on the forming wire of machine B with gridlines showing a 1-in. length scale



3c. Single frame image of the forming jet after impingement on the forming wire of machine C with gridlines showing a 1-in. length scale



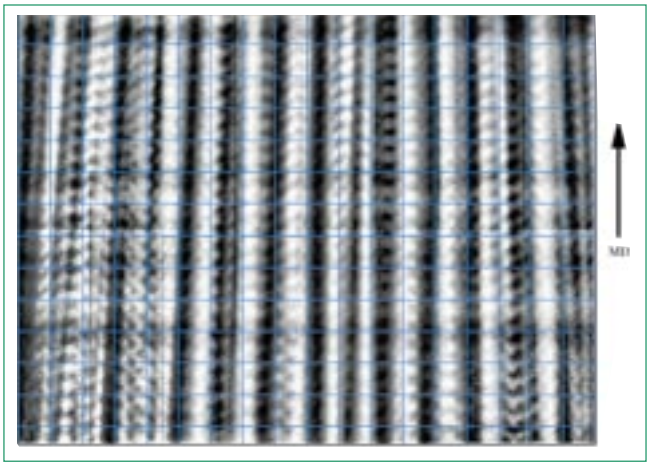
3d. Single frame image of the forming jet after impingement on the forming wire of machine D with gradlines showing a 1-in. length scale

---provided consideration of at least 100 frames—does not change the conclusions.The frequency range of interest is 0.5–2 l/in.—2–0.5 in. length scale. The dominant streaks in machines C and D are 0.5–1 in. length scale. For machines A and B, the dominant length scale is 1–2 in. In the 0.5–2 in. range, the standard deviations of machines C and D are lower than the standard deviations of images taken from machines A and B.This shows more regularity in streaks for machines C and D.

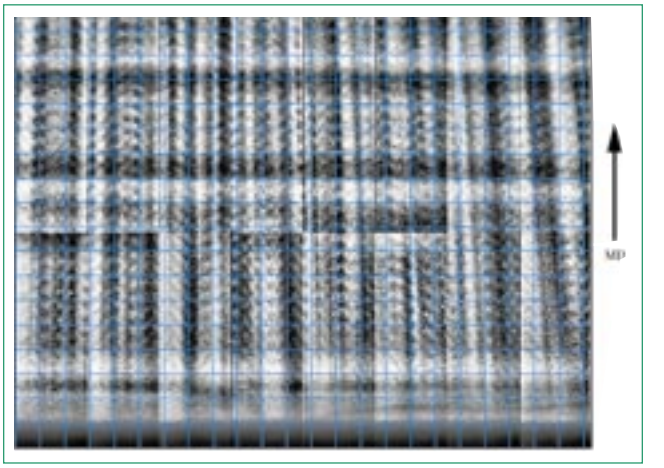
The results show that the images of the streaks for machines A and B are less regular than the streaks generated in machines C and D about the 1-in. length scale. About the 2-in. length scale, machines C and D show the most regular streak pattern. This method of comparison does not make an evaluation of the amplitude of the streaks. It only measures the persistence or regularity of the streaks. The jet impingement angle and the jet velocity strongly influence the amplitude of the streaks.

THE PHYSICS

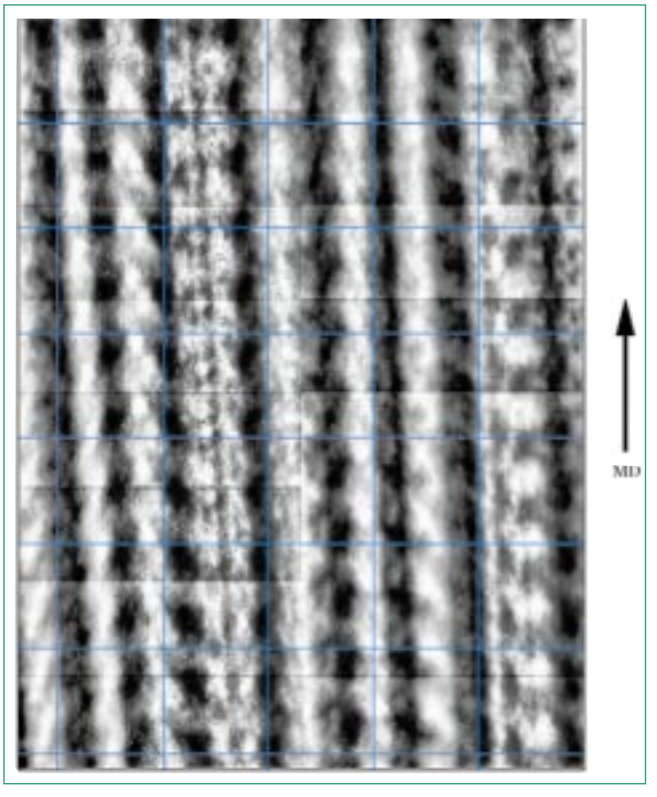
A question is why headboxes A and B deliver jets with less regular streaks than headboxes C and D in the 0.5–1 in. range. Although this work does not rigorously analyze the difference between these headboxes, some ideas are possible. The main difference between the converging nozzle of these headboxes is that both A and B have



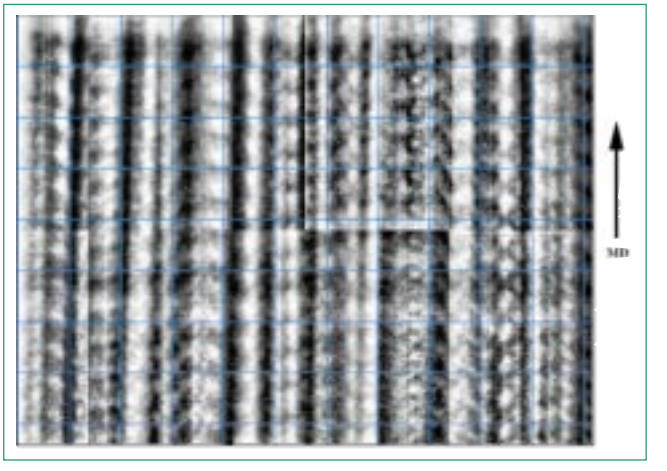
4a. Image average over 100 frames (0.1 s) of the post impingement forming layer on the forming wire of machine A with gridlines showing a 1-in. length scale



4b. Image average over 100 frames (0.1s) of the post impingement forming layer on the forming wire of machine B with gridlines showing a 1-in. length scale



4c. Image average over 100 frames (0.1 s) of the post impingement forming layer on the forming wire of machine C with gridlines showing a 1-in. length scale



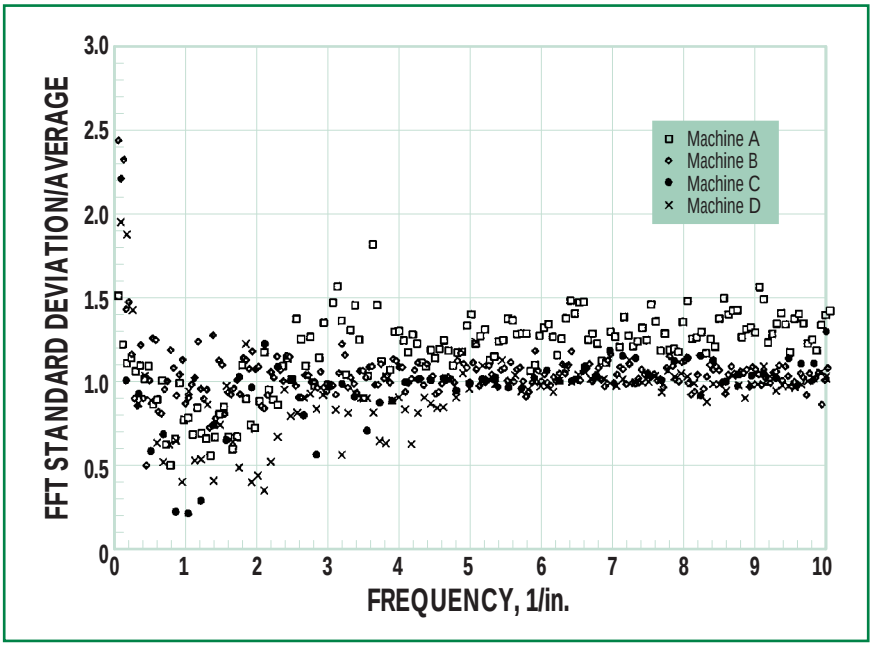
4d. Image average over 100 frames (0.1 s) of the post impingement forming layer on the forming wire of machine D with gridlines showing a 1-in. length scale

sheets extending from the tube outlet to a few inches from the slice separating the jets from each row of tubes. Headboxes C and D have no sheets. The jets from adjacent rows in headboxes C and D can therefore interact immediately starting from the outlet of the tubes. One may conjecture two mechanisms based on this difference in the converging nozzle geometry:

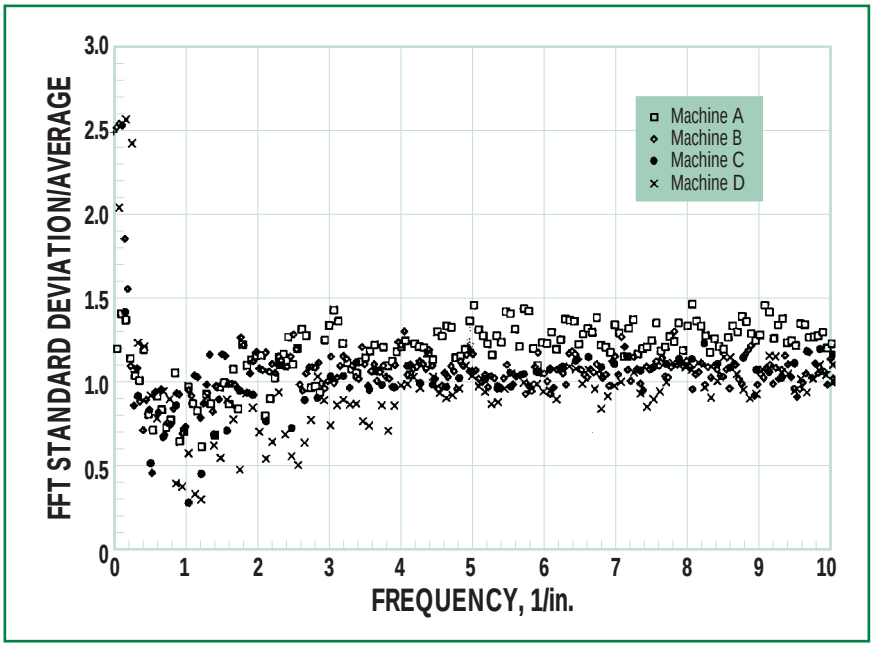
- The sheets inside the headbox provide "additional turbulence" as reported. The higher turbulent level (assuming higher turbulent level referred to in the industry is higher value for turbulent kinetic energy defined as the trace of the Reynolds stress tensor) results in damping or flattening the velocity profile from the tube jets to provide a more random jet delivered from the slice. This is probably not the mechanism since the measurements of the turbulent kinetic energy in a headbox very similar to headbox A shows an increase in the turbulent kinetic energy—most likely due to an increase in the turbulent eddy scale—by removing the sheets from the headbox *(3)*.
- The second mechanism isolates the jets from each row of tubes and therefore prevents the interaction of the tube jets with their neighbors in the rows above and below. Computational analysis of the flow

in the converging zone of the nozzle shows that a mean secondary flow of counter rotating vortices forms for each pair of jets as the jets from two rows interact *(2, 4)*. These vortices generate streaks at the slice and on the forming table. When a solid surface isolates the rows of jets, the early interaction of the jets with the adjacent jets from the rows above and below are delayed until further downstream in the converging nozzle. This changes the mechanism of interaction among adjacent jets and therefore alters the pattern of the streaks on the forming table. Considerably jagged streaks replace the straighter streaks. The jagged streaks still form along the machine direction as the averaged image in Fig. 4 a and b show. At this time, the exact mechanism for the formation of streaks in headboxes with vanes is not clear to the author who is now engaged in detailed computational analysis of a headbox with sheets and the same headbox without the sheets in the converging zone. The results of that work will appear in future publications and should provide some insight into the fluid mechanics of the forming jet by this class of headbox.

Analyzing the time line images of the forming sections presented in **Fig. 7** a–d for machines A–D, respectively, provide a further investigation of the characteristics of the forming jet from the four headboxes considered in this study. An earlier explanation provides information of time line imaging *(1)*. These images show the dynamics of the flow pattern in the forming jet. The images are taken at a section of the forming jet approximately 15 in. from the slice. The impingement line in all cases is approximately 4–6 in. from the slice.



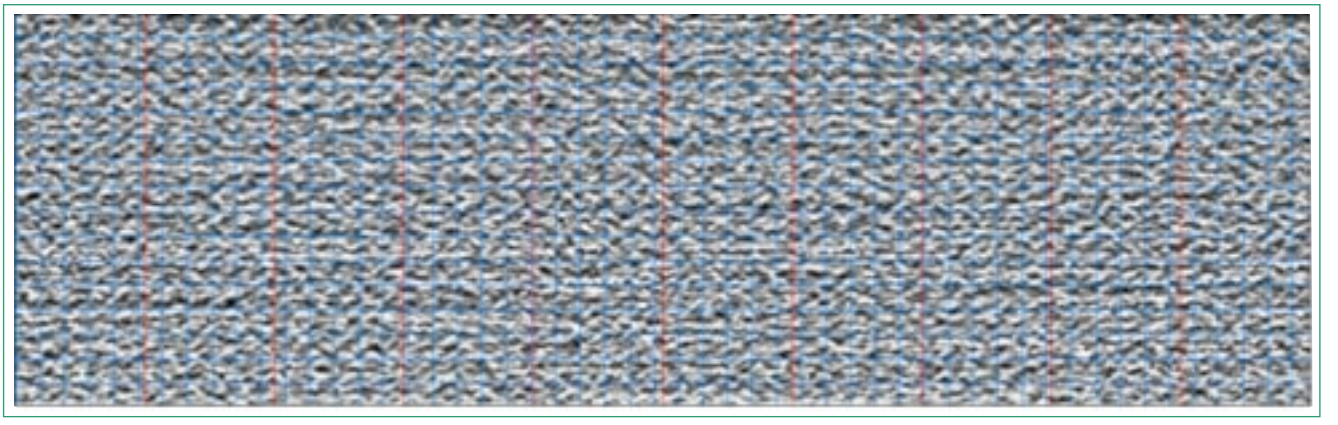
5. FFT standard deviation divided by average for all scan lines after the jet impingement for 100 frames



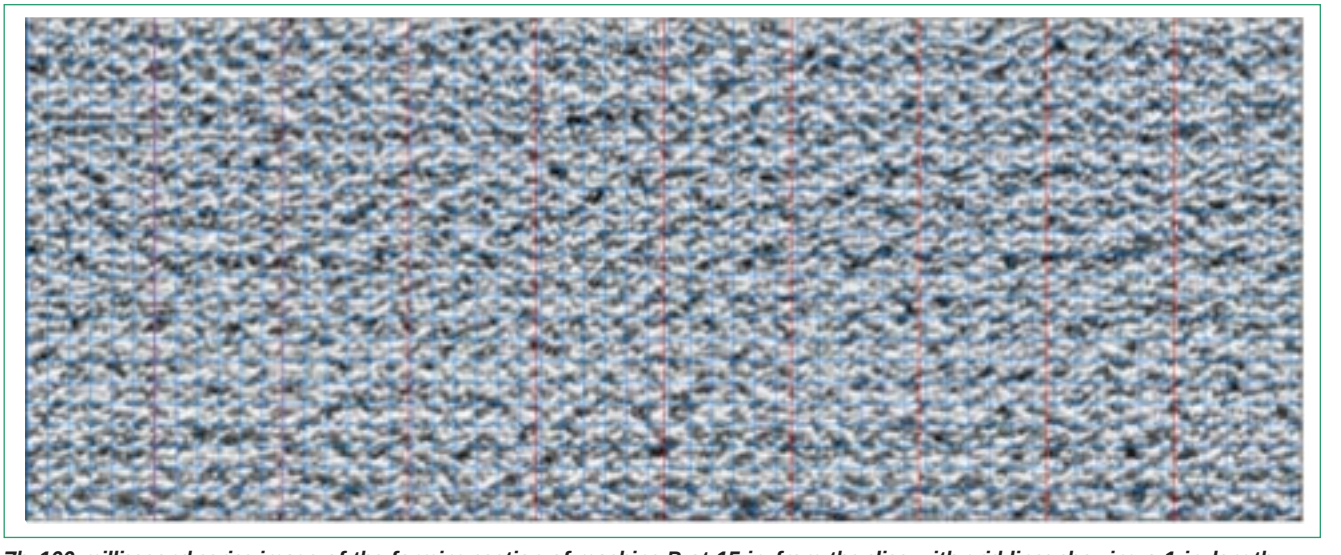
6. FFT standard deviation divided by average for all scan lines after the jet impingement for 500 frames

Machines A and B show a different surface flow pattern than machines C and D. The streaks in machines C and D have more elongation in the MD. The author hesitates to make any conclusions from visual inspection of these images.

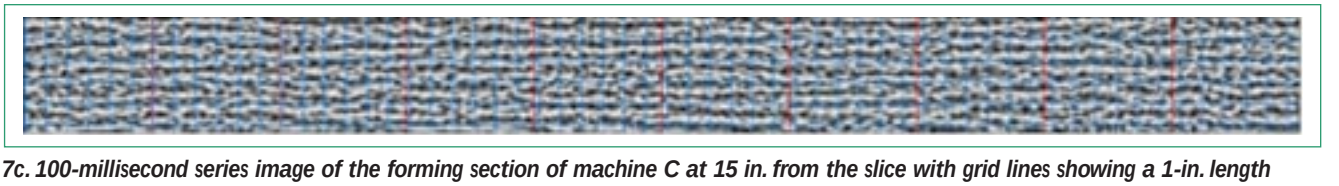
One often assumes that the smaller scale eddies in the forming layer provide a more effective mechanism for preventing fiber flocculation. Some previous studies have addressed this issue *(5–7)*. Current work at the Institute of Paper Science and Technology is investigating



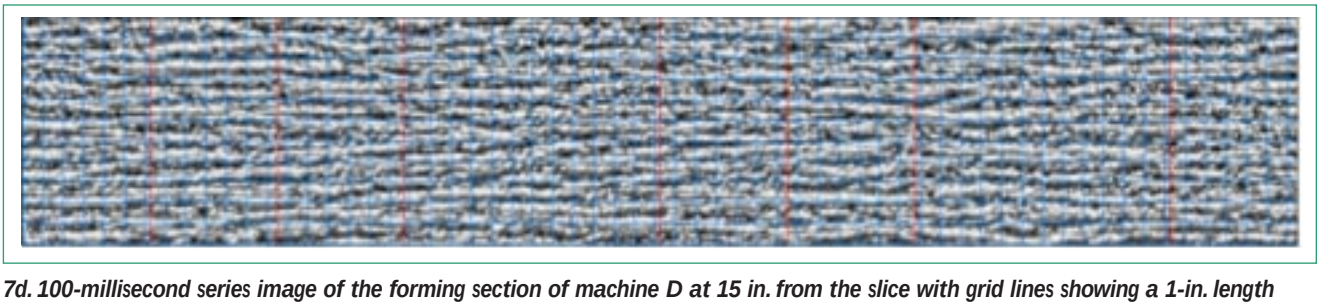
7a. 100-millisecond series image of the forming section of machine A at 15 in. from the slice with grid lines showing a 1-in. length scale and the sections bounded by lines representing a 10-millisecond increment



7b. 100-millisecond series image of the forming section of machine B at 15 in. from the slice with grid lines showing a 1-in. length scale and the sections bounded by lines representing a 10-millisecond increment



7c. 100-millisecond series image of the forming section of machine C at 15 in. from the slice with grid lines showing a 1-in. length scale and the sections bounded by lines representing a 10-millisecond increment



7d. 100-millisecond series image of the forming section of machine D at 15 in. from the slice with grid lines showing a 1-in. length scale and the sections bunded by lines representing a 10-millisecond increment

the effect of turbulent eddy structure on fiber dispersion. TJ

Aidun is professor at Institute of Paper Science and Technology, 575 14th St., NW, Atlanta, GA 30318.

Acknowledgment: Partial support for this work came from the National Science Foundation through grant CTS-9258667 and from the member companies of the Institute of Paper Science and Technology.

Received for review June 13, 1997.

Accepted Sep. 3, 1997.

Presented at the TAPPI 1997 Engineering and Paper- makers: Forming Bonds for Better Papermaking Conference.

LITERATURE CITED

1. Aidun, C. K. and Ferrier, A., *TAPPI 1997 Engineering and Papermakers: Forming Bonds for Better Papermaking Conference Proceedings*, TAPPI PRESS, Atlanta, p. 883.
2. Aidun, C. K., *TAPPI 1996 Engineering Conference Proceedings*, TAPPI PRESS, Atlanta, p. 209.
3. Kovacs, A., Roberts, P., and Aidun, C., *Report to the Georgia Consortium*, IPST, Atlanta, 1998, pp. 276–285.
4. Aidun, C. K., *Tappi J.* 79(6):55(1996).
5. Hauptmann, H., Vyse, R. and Mardon, J., *Pulp & Paper* 91(9):T357(1990) and 91(10):T369 (1990).
6. Wrist, P. E., *Formation and Structure of Paper—2*, British Paper and Board Makers Assoc., London, 1962, p. 839.
7. Lindqvist, L., "Structure in the flow from paper machine headboxes," Licentiate thesis, Lulea University of Technology, Lulea, Sweden, 1996.